Fermi National Accelerator Laboratory

FERMILAB-Conf-92/276

The DØ Upgrade

P. Michael Tuts
for the DØ Collaboration

Fermi National Accelerator Laboratory
P.O. Box 500, Batavia, Illinois 60510

October 1992

Presented at the *3rd International Conference on Advanced Technology and Particle Physics*, Como, Italy, June 22-26, 1992

Disclaimer

The D0 Upgrade

P. Michael Tuts for the D0 Collaboration*

Physics Department, Columbia University, New York, NY 10027, USA

In this paper we describe the upgrade plans of the D0 detector at Fermilab.

1. INTRODUCTION

The original D0 detector[1] was proposed in 1983, with a focus on high p_T physics using precision measurements of e's, μ's, jets, and missing E_T. This detector, as of the summer of 1992, has started data taking at the Fermilab Collider. However, by 1995/6 the luminosity will reach 10^{31} $cm^{-2}sec^{-1}$, and the minimum bunch spacing will drop to 396ns from the present 3.5μs (by the Main Injector era, luminosities will approach 10^{32} $cm^{-2}sec^{-1}$ and minimum bunch spacings may reach 132ns). These changes in the accelerator conditions force us to upgrade or replace a number of detector subsystems in order to meet these new demands. In addition, the upgrade offers us the opportunity to expand the physics horizons to include not only the all important high p_T physics menu, but also the low p_T physics that has become increasingly important. In the following sections we describe the D0 detector upgrade ($D0_\beta$). The upgrade is described in more detail elsewhere.[2]

2. PHYSICS GOALS

The physics goals of $D0_\beta$ include the full high p_T physics menu of the present D0 detector ($D0_\alpha$): top, electroweak, QCD, new particle searches, and bottom physics. In most of these areas, the upgrade will provide significant benefits. Some examples of the physics capabilities are given in the following sections.

2.1. Top Physics

The discovery and precision measurement of the top mass provides a most promising way to constrain the Standard Model and restrict the range of Higgs masses. The dilepton (from the leptonic decay of the Ws from the t-quark decays) plus jets channel, and the single lepton (from just a single leptonic decay of the W) plus jets channel are the principal discovery modes. The background from W production can be significantly reduced by b-jet tagging using their non-zero decay lengths. Studies[3] that assume 50% tagging efficiency and require at least 40 lepton plus jet events and 5 dilepton events lead to discovery limits of 165, 195, and 235 GeV for integrated luminosities of 100, 250, and 1000 pb^{-1} respectively. $D0_\beta$ studies have found 70% tagging efficiencies for a 5σ significance on the non-zero decay length.

Studies have shown that the top mass resolution due to jet energy measurements and to neutrino momentum uncertainties is 25-30 GeV/c^2, thus a 5 GeV/c^2 (statistical) mass measurement of the top mass can be achieved with a sample of about 50 lepton plus jets events. For larger samples, systematic errors will predominate. The b-tagging capabilities of $D0_\beta$ will reduce the asymmetric tails of the top mass distribution and reduce systematic errors to the level where $\delta M_{top} \cong 5$ GeV/c^2 is achievable.

2.2. Electroweak Physics

The upgrade will allow a number of precision electroweak measurements to be made, which when combined with the top mass measurement will allow a stringent test of the Standard Model. Once again, systematic uncertainties will dominate. Systematic uncertainties in W production and decay can be studied from the large sample of $Z \rightarrow e^+e^-$ events. Additional progress in understanding the parton distributions (*e.g.* the proton u/d ratio) will reduce to 25 MeV that contribution to the uncertainty, allowing an overall error of $\delta M_W \cong 50$ MeV to be achieved.

Proceedings of the 3rd International Conference on Advanced Technology and Particle Physics, Como, Italy, 22-26 June 1992

The inner solenoidal magnetic field in $D0_\beta$ will allow a sign determination for both electrons and muons. Thus the upgraded detector will provide a LEP-competitive determination of A_{FB}, the forward-backward asymmetry between the e^+ from a Z and the initial proton direction. A 1 fb^{-1} sample of data would lead to an error of less than 1% for $\sin^2\theta_W$.

2.3. Bottom Physics

The very large sample of b pairs produced in a $1fb^{-1}$ sample ($\cong 5\times10^{10}$) provide the required data to carry out studies of B production which are necessary to understand B decay, mixing, and ultimately CP violation. The large solid angle coverage for μ's (down to $|\eta|=3$), the capability to trigger at small angles (provided by the small angle muon system upgrade), and the forward silicon tracking system are the tools with which to access the data.

Some of the physics goals in this area include studies of B_c decays (about 6×10^7 are produced) through decays such as $B\rightarrow\Psi\mu\nu$ ($BR\cong 5\times10^{-4}$). Rare B decays are also accessible with such data samples. Our studies have also shown that B_s mixing, which is expected to be considerably larger than in the B_d system, can be measured using $B_s\rightarrow D_s\pi\pi\pi$, $D_s\rightarrow\phi\pi$ decays to reconstruct the B_s, together with cuts on the decay length significance, which are provided by the silicon tracker system. An ultimate goal would be the search for CP violation. Our studies of $B^0\rightarrow\Psi K_s\rightarrow\mu\mu\pi\pi$ decays have shown that the error we might achieve on the CP violating angle, $\sin2\beta$, is about 0.15, which is four times smaller than the present upper limit. A measurement of the CP violating dilepton asymmetry is difficult (requiring a greater than 6% efficiency), but perhaps within reach.

3. THE D0 UPGRADE

The upgrade of the present, and running, D0 detector (refereed to as $D0_\alpha$) is driven by two principal needs. The first is to accommodate changes in the accelerator environment including higher luminosity (from 10^{30} to $5\times10^{31}cm^{-2}s^{-1}$) and shorter times between beam bunches (from 3.5μs to 396 ns minimum bunch spacing). Thus we face the general problem that crossing times become smaller than drift and shaping times, and that the high luminosities raise the issues of radiation damage and pile-up. The second is a change in the physics opportunities in the late 1990s, where we expect a shift from discovery to precision measurements, and the blossoming of B physics at hadron colliders (as demonstrated by CDF). Fortunately, technological advances let us tackle both of these issues. In the following sections we describe the D0 upgrade detector.

Present schedules indicate that Fermilab will increase the number of bunches in the machine from 6x6 to 36x36 for collider Run II (late 1995), with the highest luminosities reached in the Main Injector Run III ($\cong$1998). At the very highest luminosities, a 99x99 bunch structure may be adopted, corresponding to 132ns minimum bunch spacing. The D0 upgrade is phased to accommodate these anticipated schedules.

3.1 Calorimeter

The D0 uranium-liquid-argon calorimeter is intrinsically radiation hard, however the shorter bunch spacing introduces a number of problems for the calorimeter signals. The present calorimeter electronics has been optimized to accommodate the noise contributions from (1) electronics, (2) uranium, and (3) pile-up. We presently have an effective shaping time of 2.2μs. A baseline is measured before every crossing and subtracted from the peak signal value taken 2.2μs later.

The upgrade of the calorimeter electronics requires (1) a re-optimization of the shaping time, (2) the addition of a delay in the signal path to accommodate the trigger formation time of $\cong$2μs, and (3) a change in the timing of the baseline measurement. Thus we propose to shorten the shaping time of the preamp from $\cong$2.2μs to $\cong$400ns (using a unipolar Sallen-Key filter). The effect of the shorter shaping times is to increase electronic noise and decrease the uranium and pile-up noise. To compensate for the increase in electronic noise we will replace all preamps with lower noise (2 JFETs on the input) devices. A 2μs delay will be added in the shaper circuitry to cover the trigger formation time. The present design calls for a lumped parameter delay line; other options are being investigated. The baseline sampling will occur in the $\cong$2.6μs interval between the three 12-bunch superbunches.

The response of the system for a precision W mass measurement has been simulated. This is perhaps the most stringent test of calorimeter performance. Our studies indicate that the performance of the new electronics at the highest expected luminosity at Fermilab of $5\times10^{31}cm^{-2}s^{-1}$ (36×36 bunches) is equivalent to the expected performance of the present electronics at a luminosity of $10^{31}cm^{-2}s^{-1}$ (6×6 bunches). The pile-up, from an average of 2 events per crossing, degrades the resolution by ≅15%, and contributes ≅100-200 MeV to a systematic shift in the W mass. The W mass shifts can be studied using Z events. These conclusions remain essentially unchanged even for the shortest bunch spacings contemplated for Fermilab of 132ns (99×99 bunches).

3.2 Muon System

The muon PDT system faces problems similar to the calorimeter system, namely that the drift times will be larger than the bunch spacing time. In addition, the increase in the number of bunches will increase the cosmic ray rate unless tighter timing windows are implemented. There are a number of areas where the muon system will be upgraded.

Faster charge collection time will aid in trigger formation, thus we will replace the large angle muon PDT gas with a faster gas ($ArCO_2CF_4$). This should lower the drift time from ≅1.2μs to ≅800ns.

Since the drift time will still be greater than the crossing time we will need to tag every event of interest with a time-stamp associated with a crossing number. This will be achieved by providing full scintillator coverage of the muon PDTs. Scintillator sheets, matched to the PDT sizes, with wave shifter fiber readout will provide a time stamp to within a 20ns window. The wave shifter fibers will be placed in grooves in the scintillator and read out by photo multiplier tubes. In this way we achieve full and efficient coverage. The present detector uses acrylic scintillator with wave shifter bar readout on the top of the detector only.

The increased luminosity will put severe strains on the small angle muon system (SAMUS) for both detection and triggering. However it is crucial for D0 to maintain the full muon coverage it presently has, thus we will provide a small cell chamber in that region to deal with the luminosity increases. These two dimensional chambers will provide the necessary granularity to trigger on small angle μ's.

The increased rates in the SAMUS will require improvements to the muon electronics including (1) double hit capability for drift time measurements, (2) increased spatial resolution at the trigger level, and (3) an increase in the digitization speed.

3.3 Trigger and DAQ

The basic trigger problem is evident. The raw rate will increase by about two orders of magnitude (5MHz at a luminosity of 10^{32}) over the original design luminosity. Some of the upgrades are well defined, and involve expanding the number and complexity of the Level 1 (dead time-free) trigger system. The bandwidth into Level 2 (microprocessor farm) will be increased by using additional data paths. The throughput will be increased from about 400Hz to 1KHz. The increased load in Level 2 will be addressed by using more powerful processors and/or co-processors. The output rate from Level 2 will be increased from 2Hz to about 10Hz. In addition to these relatively straightforward upgrades, we anticipate the need to incorporate fiber trigger options, more sophisticated calorimeter triggers, correlations across different detector systems. The precise form and requirements for these triggers will require us to gain experience with the existing system.

3.4 Tracking System

A major component of the D0 upgrade is the full replacement of the present tracking system that consists of a jet cell vertex drift chamber (VTX), a TRD, and an outer jet cell drift chamber (CDC). The small angle regions are covered by forward drift chambers (FDC) that provide θ and φ coordinates. These relatively large drift cell devices will suffer from event pile-up at high luminosities, and after a one year run at luminosities of 10^{31} they will have accumulated 1 C/m of charge on the innermost wires and will start to show a performance degradation.

The replacement system will consist of an inner silicon micro strip tracker surrounded by a scintillating fiber tracker inside a solenoidal magnetic field. Surrounding the superconducting coil will be a preshower detector. A schematic view of the tracking system is given in Fig. 1. This system will

allow for operation at $10^{32}cm^{-2}s^{-1}$ with 132ns beam crossing, measurement of $\Delta p/p$ over $|\eta|<3$ with sufficient accuracy to determine the sign of the charge of electrons and to reconstruct exclusive B decays, good pattern recognition for isolated particles, and sufficient vertex resolution to identify B decays near jets. The tracker will enhance the identification of electrons in the calorimeter through E and p comparisons, and by extrapolating candidate tracks into the preshower.

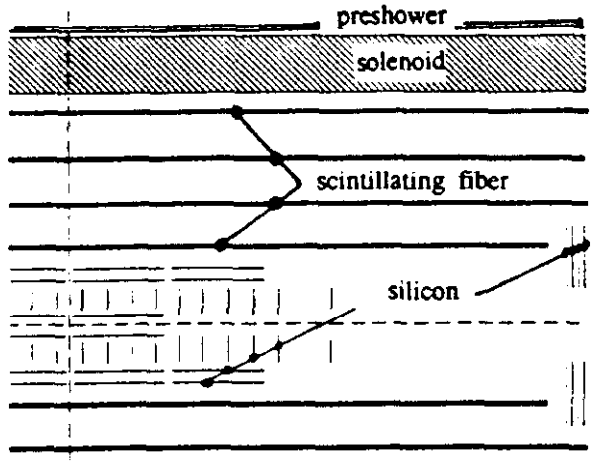

Fig. 1 *Schematic side view of ≡1/4 of* $D0_\beta$ tracking system.

3.5 Solenoidal Magnet

The superconducting solenoidal magnet for the D0 upgrade is required to have the following specifications: radius less than 72cm, 2T field, uniform to better than 2% for $|z|<0.8$m, thickness <16cm and radiation length $<1X_0$, length of 2.6m. The requirements are modest are not expected to pose any unusual technical challenges.

3.6 Silicon Tracking System

The silicon tracker system consists of a 3-layer Si barrel and 28 Si disks. The geometry is driven by the large σ=30 cm interaction region. Each barrel layer is constructed from 6×3.2 cm^2 single sided Si detector planes, with strips of 50μm pitch along the 6 cm (axial) direction. One logical unit consists of two detectors ganged together into 12×3.2 cm^2 segments, and two logical units comprise a ladder. The outer two layers (at r=11.9 cm and 14.9 cm) consist of four ladders (96 cm total length), and the innermost layer (at r=2.7 cm) consists of two ladders (48 cm long). The disk system consists of three styles (E, F, and H) which provide coverage to η=3. The E, F disks are similar (see Fig. 2), consisting of twelve 2-sided wedge detectors on which the 50μm pitch strips run parallel to one of the radially extending edges on one side, and parallel to the other edge on the other side. This geometry provides 30^0 stereoscopic space point measurement. The E and F disks only differ in their inner radius of 4.1 cm and 2.6 cm respectively, the outer radius is 10cm in both cases. The H disks cover the radial region from 9.5 cm to 26 cm with single sided 90^0 stereo angle devices.

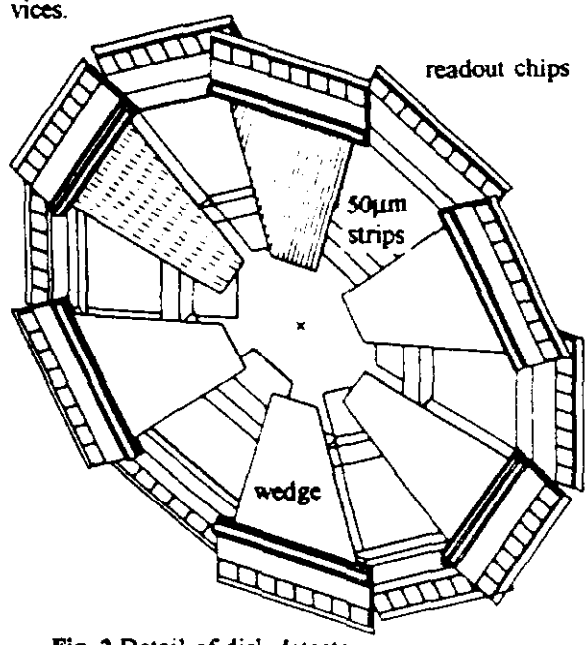

Fig. 2 Detail of disk detector.

The readout consists of 128 channel AC-coupled SVX-II-type readout chips with onboard digitization. Each side of a wedge detector requires 8 such chips mounted at the outer radius. A readout sector consists of four (eight) such assemblies in the barrel (disk) region. Each set of assemblies is multiplexed and controlled through a port card, these signals are passed to a second-level multiplexer and converted to optical signals. The 700W cooling load will be handled by a near-turbulent sub-atmospheric pressure water system. The full system consists of 937K silicon channels.

3.7 Scintillating Fiber Tracking System

The scintillating fiber tracking system consists of four fiber barrel systems at r=20, 31.5, 43, and 54 cm. The outer three barrels are 2.8m long and the innermost one is 2.6m long. Each of the four barrels consists of an 8-fiber-deep superlayer structure. A super layer consists of 4 layers of axial fibers and two layers each of stereo fibers. The scintillating fibers are 835μm in diameter (including a thin 25μm thick acrylic cladding), and use 1% p-Terphenyl, 1000ppm 3HF to provide reasonably fast (5-7ns) scintillator light peaking at 530nm. The fibers are coupled to clear wave guides 6-7m long, which bring the signals to the photo detectors. The full system consists of 86,000 fibers.

The readout device for the scintillating fibers must be a high QE, high gain device in order to detect minimum ionizing particles. Using these devices we can expect worst case photoelectron yields of about 5 p.e. (at η=0) after being readout with 7m of clear wave guide. The visible light photon counter (VLPC) being developed by Rockwell[4] is just such a device. They exhibit high QE of >60%, and they operate at cryogenic temperatures (6-8K). A beam test at BNL has shown the viability of the system, and a large scale cosmic ray test (≅3,000 channels) will be conducted this winter at Fermilab. An order for 5,000 channels of VLPC has been placed with Rockwell.

3.8 Preshower Detector

The preshower detector is located directly outside the coil, and consists of a tapered lead absorber (to provide a constant $2X_0$ radiator when combined with the coil material) plus six layers of scintillator sheet with wavelength-shifting (WLS) fiber readout. The layers are organized in a *zzuuvv* arrangement with a *uv* stereo angle of $\pm 10^0$. A sketch showing a section through two of the layers is shown in Fig. 3. The readout system is the same VLPC system described above.

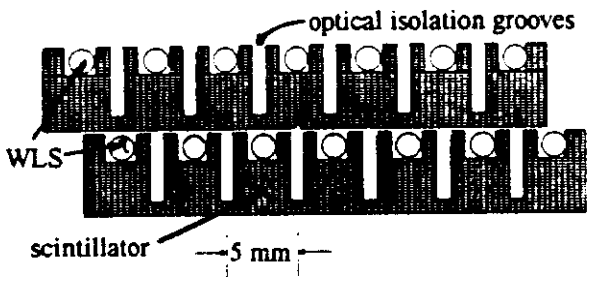

Fig. 3 Preshower scintillator geometry showing two staggered layers and optical isolation grooves.

4. TRACKING PERFORMANCE

Extensive simulation work and measurements have been carried out on the performance of the upgrade tracking system. Some results are presented below.

4.1 Signing Significance

The solenoid provides a measurement of the lepton sign over much of the solid angle, as shown in Fig. 4. In particular, the sign determination for the leptons from Z decay can be made up to $\eta \cong 3$.

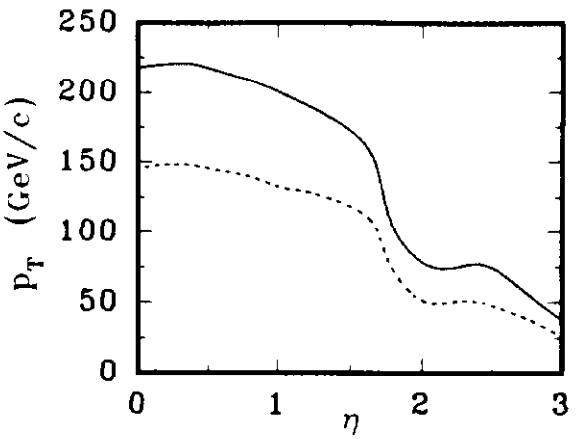

Fig. 4 Limits at the 2σ (solid) and 3σ (dashed) level for the determination of the sign of charged particles vs η.

4.2 Vertexing

The ability to use the tracker to reject backgrounds in B decays of interest ($B \rightarrow \psi K_s$, $\psi \rightarrow \mu\mu$) is demonstrated in Fig. 5. It shows the distribution of the significance of the decay length (DL), DL/δ(DL), in units of standard deviations for those decays. A modest 5σ cut on the vertex displacement preserves ≅70% of the signal.

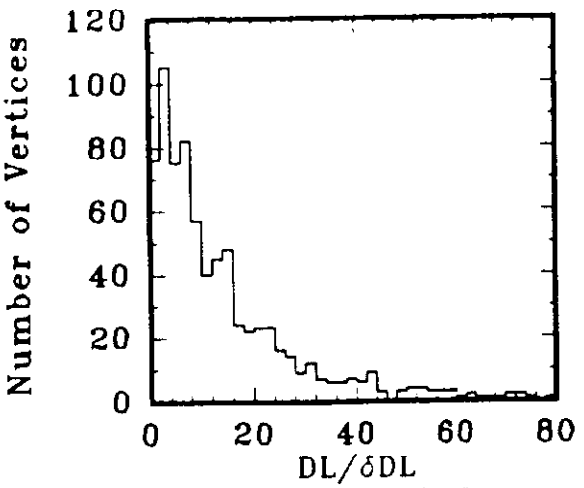

Fig. 5 Decay length significance for $B \to \psi K_s$, $\psi \to \mu\mu$ events.

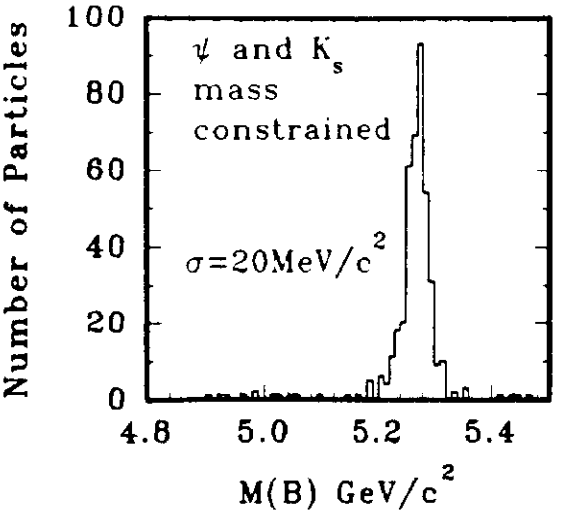

Fig. 7 Reconstructed B mass in $B \to \psi K_s$ decays, with ψ and K_s mass constrained.

4.3 Resolutions

The silicon strips can provide resolutions of about 10μm, and the fibers have been measured to provide resolutions, for a doublet of fibers, of ≅110μm. The first simulations of the full pattern recognition (silicon + fibers) at 2T field indicate that the resolution, $\delta p_T/p_T$, has a σ=0.06 for the μ's from $Z \to \mu\mu$ decays (see Fig. 6).

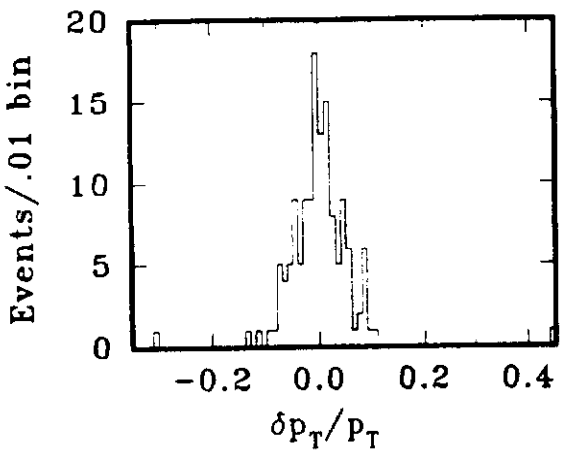

Fig. 6 $\delta p_T/p_T$ for the μ's from $Z \to \mu\mu$ decays

The effective mass measurement resolution with the upgrade is improved to the level necessary to carry out B physics. A study of $B \to \psi K_s$ decays achieves a B mass resolution of 20 MeV with ψ and K_s mass constraints (or 73 MeV unconstrained), as shown in Fig. 7. This is sufficient to reject potential backgrounds such as $B \to \psi K_s \pi^0$.

The effect of the energy loss in the dead material of the coil and the impact of the field has been simulated. There is no observable influence of the field on the jet energy resolution, or the electromagnetic energy resolution after using the preshower detector to correct for the energy losses. Figure 8 shows a

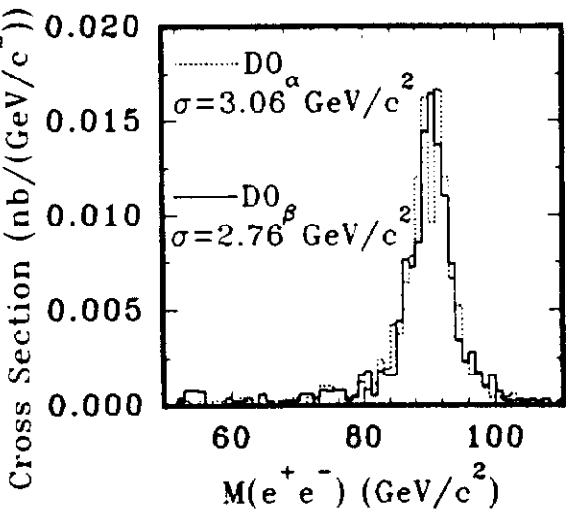

Fig. 8 Mass resolutions for $Z \to ee$ events for the present $D0_\alpha$ (dashed) and $D0_\beta$ (solid) with preshower corrections.

comparison of mass resolutions from $Z \rightarrow ee$ events for the present $D0_\alpha$, and for $D0_\beta$ with preshower corrections.

4.4 Tracking Robustness

We have studied the pattern recognition robustness by comparing the track finding efficiency for $Z \rightarrow \mu\mu$ and $t\bar{t} \rightarrow \mu$'s vs the fiber (or VLPC) inefficiency (*i.e.* turning off a fraction of random fibers). Since the algorithm is still being studied, the absolute efficiencies may not yet be optimized, but the efficiency losses indicate the intrinsic robustness of the silicon-scintillating-fiber tracking system. There is no catastrophic loss of efficiency even with 10% of the channels dead, as shown in Fig. 9. Occupancies are manageable, for $t\bar{t} \rightarrow l$+*jets* they range from 8% in the innermost layers to 2.5% in the outer layers.

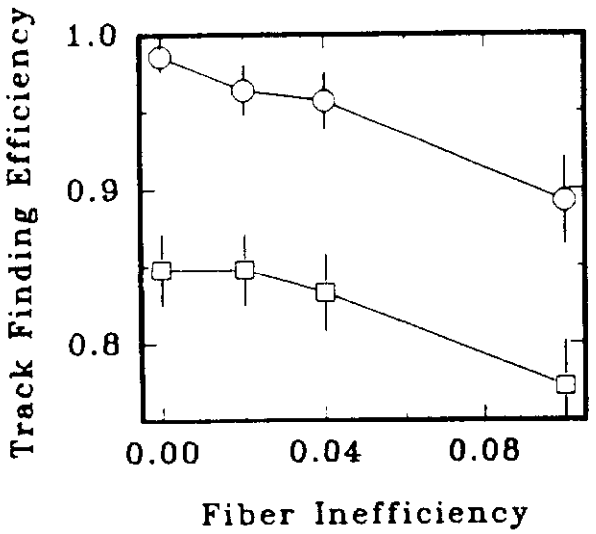

Fig. 9 Track finding efficiency for $Z \rightarrow \mu\mu$ and $t\bar{t} \rightarrow \mu$'s vs the fiber (or VLPC) inefficiency.

4.5 Electron Identification

The magnet and the preshower must replace the electron identification abilities of the present TRD. The performance of a preshower of the type outlined above has been tested in a beam. Based on the cluster pulse height, one can achieve pion rejection factors from 86-98% with electron efficiencies of 85-100% for energies from 10-100 GeV respectively. The cluster pulse height distribution for 10 GeV incident pions and electrons is shown in Fig. 10.

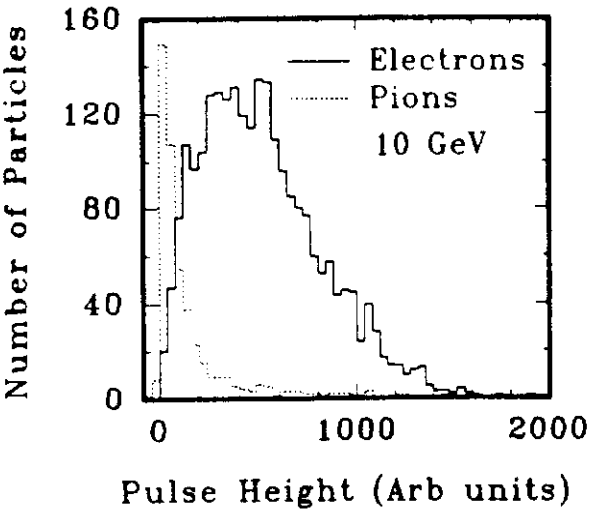

Fig. 10 Measured pulse height distribution (after clustering) in a preshower test module exposed to 10 GeV electrons and pions.

A high statistics study was used to determine the number of false electrons that are found for a variety of processes of interest (QCD, $Z \rightarrow ee$, $t\bar{t}$, $B\bar{B}$) after applying E/p and preshower criteria. Out of 10^6 QCD events analyzed, 1244 false electrons are found, with the preshower cuts effective at lower p_T and $|\eta|<1.4$, and the E/p cuts effective at larger p_T and smaller angles.

Another possible source of misidentification electrons are photons that have converted near the interaction region (in the beam pipe or first few detectors). These conversions can arise from π^0 decays in multi-jet events in which one photon is semi-isolated, or from direct photon events which primarily yield isolated high p_T electrons. The first background was simulated, the second estimated from recent CDF results. Our studies find that this background does not dominate the W and Z cross section to electrons (see Fig. 11). This study did not take advantage of better rejection that might be achieved by the opening up of the electron-positron pair in the magnetic field.

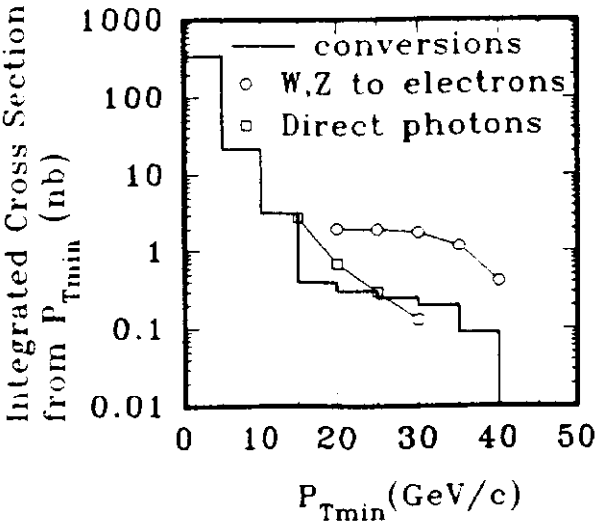

Fig. 11 Integrated cross section for conversions (isolated π^0), together with cross section for W and Z to electrons, and direct photon conversions.

5. STATUS OF THE UPGRADE

The upgrade is envisioned to be built in steps. The first stage implements all the necessary changes to accommodate the 396ns bunch spacing, and replace the VTX, which is expected to be noticeably degraded. Therefore, Step 1 consists of the upgrades to the calorimeter electronics, the muon scintillator, muon electronics, some parts of the trigger/DAQ, a 200K channel silicon tracker (3 barrels and 6 disks), a 17K scintillating fiber system consisting of two barrel superlayers located inside the TRD radius of 17 cm. Step 1 is targeted for completion by the start of Fermilab Run II (late 1995). With the exception of the scintillating fiber tracker, all of the above upgrades have been approved by Fermilab. The scintillating fiber tracker awaits the results of the large scale test.

The remainder of the upgrade: full silicon and scintillating fiber tracker, the superconducting solenoid, the preshower detector, the small angle muon system, and the full trigger/DAQ are expected to be complete by the 1997 Fermilab collider run.

ACKNOWLEDGMENTS

A project of this magnitude can only be carried out by a large team of individuals. I wish to thank all my D0 colleagues for their contributions to this effort. I also wish to thank the organizers for an enjoyable conference despite the rain. This work is supported in part by the US National Science Foundation.

REFERENCES

* The D0 collaboration: Universidad de los Andes, Bogota, Colombia; University of Arizona, Brookhaven National Laboratory; Brown University; University of California, Riverside; Centro Brasiliero de Pesquisas Fisicas, Rio de Janeiro, Brazil; CINVESTAV, Mexico City, Mexico; Columbia University; Delhi University, Delhi, India; Fermilab; Florida State University; University of Hawaii; University of Illinois, Chicago; Indiana University; Iowa State University; Lawrence Berkeley Laboratory; University of Maryland; University of Michigan; Michigan State University; Moscow State University, Russia; New York University; Northeastern University; Northern Illinois University; Northwestern University; University of Notre Dame; Panjab University, Chandigarh, India; Institute for High Energy Physics, Protvino, Russia; Purdue University; Rice University; University of Rochester; CEN Saclay, France; State University of New York, Stony Brook; Superconducting Supercollider Laboratory; Tata Institute of Fundamental Research, Bombay, India; University of Texas, Arlington; Texas A&M University.

[1]D0 Design Report, Nov. 1984 (unpublished).

[2] D0 Upgrade proposal (10/18/90); D0 note 1148 (6/18/91); D0 note 1322 (1/13/92); D0 note 1426 (5/20/92).

[3]Fermilab Program through 1997 and Beyond, report to the 1992 HEPAP subpanel (Feb. 1992).

[4]M. Petrov, contributed paper to this conference; M. Atac, contributed paper to this conference.